A complex modulated magnetic structure in $CeNi_2Al_5$ persisting at very low temperatures

1999 J. Phys.: Condens. Matter 11 7327

(http://iopscience.iop.org/0953-8984/11/38/311)

J. Phys.: Condens. Matter **11** (1999) 7327–7338. Printed in the UK PII: S0953-8984(99)02687-9

A complex modulated magnetic structure in $CeNi_2Al_5$ persisting at very low temperatures

F Givord†‖¶, J-X Boucherle†¶, J Dreyer†, Y Isikawa‡, B Ouladdiaf§, S Pujol§, J Schweizer† and F Tasset§

† Département de Recherche Fondamentale sur la Matière Condensée, SPSMS-MDN, CEA/Grenoble, 38054 Grenoble Cédex 9, France
‡ Department of Physics, Toyama University, Toyama 930, Japan
§ Institut Laue–Langevin, BP156, 38042 Grenoble Cédex 9, France

E-mail: givord@drfmc.ceng.cea.fr

Received 17 March 1999, in final form 24 June 1999

Abstract. The orthorhombic compound $CeNi_2Al_5$ is magnetically ordered below 2.6 K. Kondo-type interactions together with strong crystal-electric-field (CEF) effects give rise to a complex magnetic structure: (i) its propagation vector is three dimensional and incommensurate, $\boldsymbol{k} = (0.500, 0.405, 0.083)$; (ii) the Fourier components of the moment associated with this vector are tilted away from the easy-magnetization axis $\boldsymbol{b}$. Furthermore, the magnetic structure is double $\boldsymbol{k}$, as the propagation vectors $\boldsymbol{k} = (k_x, k_y, k_z)$ and $\boldsymbol{k}' = (-k_x, k_y, k_z)$ associated with different magnetic domains are not independent.

New experiments have been undertaken to achieve a more precise determination of the magnetic structure. Magnetic peak intensity measurements with higher resolution and polarization analysis have both led to the conclusion that the Fourier component of the magnetic moment deviates slightly from the $\boldsymbol{b}$-direction. Considering the coupling of the two propagation vectors, the resulting moment describes very flat ellipses with most of the moments very close to $\boldsymbol{b}$. Neutron diffraction experiments down to 0.4 K have also been performed to investigate the evolution of the magnetic structure at low temperatures.

1. Introduction

$CeNi_2Al_5$ is a dense Kondo compound [1, 2] with a magnetic transition at 2.6 K. The temperature dependence of its resistivity is typical for the presence of the Kondo effect: it exhibits a minimum at around 30 K, followed by a $-\ln T$ behaviour as temperature decreases and a maximum at around 4 K. The abrupt drop of the resistivity, the magnetic susceptibility and the specific heat confirm the transition to an antiferromagnetic-type ordering below $T_N = 2.6$ K. Due to the Kondo effect, the entropy at T_N is reduced to 75% of $R \ln 2$ and reaches the full value only at 8 K. The crystal structure of $CeNi_2Al_5$ (figure 1) is body-centred orthorhombic [3, 4] (space group: $Immm$), with lattice parameters $a = 7.045$ Å, $b = 9.637$ Å, $c = 4.015$ Å [1]. The cerium atoms are all located at (0 0 0) and (1/2 1/2 1/2) positions, which correspond to one unique crystallographic site in the primitive unit cell. The orthorhombic local symmetry leads to strong crystal-electric-field (CEF) effects and a very large anisotropy has been observed. In fact, magnetization curves, measured along the three principal symmetry directions [5],

‖ Author to whom any correspondence should be addressed; telephone: 04 76 88 58 65; fax: 04 76 88 51 09.
¶ CNRS staff.

0953-8984/99/387327+12$30.00

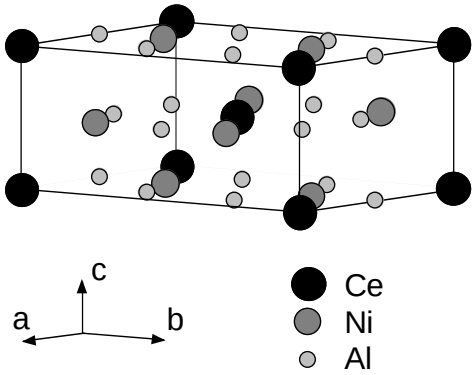

Figure 1. Crystal structure of $CeNi_2Al_5$.

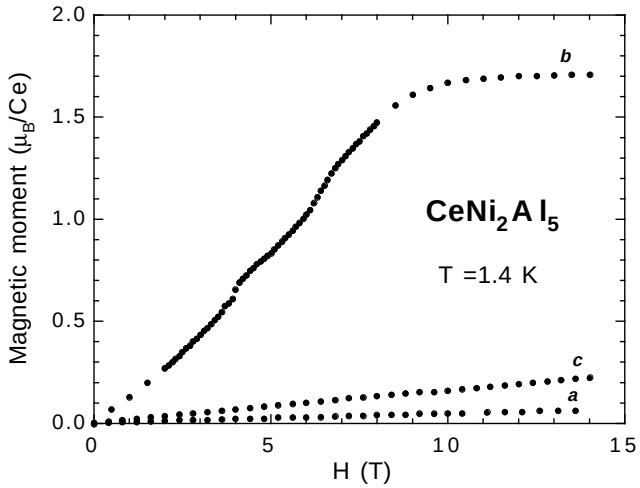

Figure 2. Magnetization curves of $CeNi_2Al_5$ single crystal at 1.4 K up to 14 T.

show a very large anisotropy with $\boldsymbol{b}$ as the easy-magnetization axis (figure 2). In a magnetic field of 14 T, the magnetization along $\boldsymbol{b}$ reaches a maximum value of 1.7 μ_B/formula unit and those along $\boldsymbol{c}$ and $\boldsymbol{a}$ are about 10 and 20 times smaller, respectively. Inelastic neutron spectroscopy [6], together with the magnetization and susceptibility results, has allowed the determination of the CEF parameters. These values were confirmed by the analysis of the magnetic form factor [7].

The $CeNi_2Al_5$ magnetic structure at 1.5 K has been determined from neutron diffraction experiments [5, 8]. Because of the Kondo interactions, this structure is rather complex: (i) the propagation vector is three dimensional and incommensurate, $\boldsymbol{k} = (0.500, 0.405, 0.083)$, (ii) the Fourier component $\boldsymbol{m}^k$ of the moment is not oriented along the easy-magnetization direction $\boldsymbol{b}$ but is slightly tilted (8°) towards $\boldsymbol{a}$ in the $(\boldsymbol{a}, \boldsymbol{b})$ plane. This result is in contradiction with the huge anisotropy found between these two axes in the magnetization measurements. However, some low-temperature nuclear orientation experiments had already led to similar conclusions [9]: at 10 mK, the moment had been deduced to be in the $(\boldsymbol{a}, \boldsymbol{b})$ plane, at 27° from

the $\boldsymbol{b}$-axis. Furthermore, from neutron diffraction under an applied magnetic field [6, 10], it has been shown that the propagation vectors $\boldsymbol{k} = (k_x, k_y, k_z)$ and $\boldsymbol{k}' = (-k_x, k_y, k_z)$ associated with different magnetic domains are not independent and that the magnetic structure is double $\boldsymbol{k}$.

As it had been noticed that some of the magnetic reflections measured in the previous magnetic structure determination [5,8] were overlapping each other, and to clarify the direction of the Fourier component $\boldsymbol{m}^k$, it was decided to perform new experiments on the same crystal as had been previously studied. On the one hand, a new classical neutron diffraction experiment was undertaken on a four-circle diffractometer, in order to measure more satellites in the two magnetic domains. A large wavelength was used to obtain a better resolution. The evolution of the magnetic structure as temperature decreased to very low values was also looked at, especially searching for $3\boldsymbol{k}$-type satellites. On the other hand, the three-dimensional neutron polarization technique was also used to check whether $\boldsymbol{m}^k$ is aligned along the $\boldsymbol{b}$-direction or not.

2. Magnetic structure at 1.6 K

The classical neutron diffraction experiment was performed on the four-circle diffractometer D10 at ILL (Grenoble) at $T = 1.6$ K. Because of the very large value of the lattice parameter b, reflections belonging to different magnetic domains such as $(h, k, l) + (k_x, k_y, k_z)$ and $(h + 1, k + 1, l) + (-k_x, -k_y, k_z)$ are very close to each other and can overlap. We therefore used a large incident wavelength of 2.36 Å and it has been checked that the magnetic peaks were well separated from each other.

If the structure were single $\boldsymbol{k}$, with a propagation vector of type (k_x, k_y, k_z), four magnetic domains would exist in the sample, corresponding to the four equivalent vectors obtained by the orthorhombic symmetry operations of the crystal. As the structure is double $\boldsymbol{k}$, with vectors $\boldsymbol{k} = (0.500, 0.405, 0.083)$ and $\boldsymbol{k}' = (-0.500, 0.405, 0.083)$ coupled together, there are only two magnetic domains associated with $\boldsymbol{k}_1$, $\boldsymbol{k}_1'$ and $\boldsymbol{k}_2$, $\boldsymbol{k}_2'$. 184 magnetic reflections corresponding to the two domains have been measured—that is, in each domain, 46 reflections associated with the propagation vector $\boldsymbol{k}$ and 46 others associated with the propagation vector $\boldsymbol{k}'$.

2.1. Real Fourier components

As the magnetization is strongly anisotropic, the magnetic structure was first assumed to be collinear—that is, the Fourier component $\boldsymbol{m}^k$ was assumed to be real. The values of the refined [11] Fourier components associated with each propagation vector are gathered in table 1. One can notice that for a given $\boldsymbol{k}$-vector, the signs of the $\boldsymbol{m}^k$-components are well defined. In particular, for the two associated vectors $\boldsymbol{k}$ and $\boldsymbol{k}'$, where the k_x-components are opposed, the corresponding m_x^k-components are also opposed. The tilt angle of $\boldsymbol{m}^k$ away from the easy-magnetization axis $\boldsymbol{b}$ in the $(\boldsymbol{a}, \boldsymbol{b})$ plane is $\beta = \arctan(m_x^k/m_y^k)$. The reliability factors associated with the four propagation vectors are very close to each other. They are around 7%, whereas they increase to about 12% when the m_x^k-component is fixed to zero. The two domains are found to be equivalent in size. The mean values corresponding to $\boldsymbol{k} = (0.500, 0.405, 0.083)$, are the following:

$$m_x^k = -m_x^{k'} = -0.040(3)\ \mu_B$$
$$m_y^k = +m_y^{k'} = +0.591(3)\ \mu_B$$
$$m_z^k = +m_z^{k'} = 0.$$

Table 1. Fourier components $\boldsymbol{m}^k$ and tilt angle $\beta = \arctan(m_x^k/m_y^k)$ refined for each propagation vector $\boldsymbol{k}$ in each domain. The reliability factor is defined as $R = \sqrt{[\sum_i p_i(I_i^{obs} - I_i^{calc})^2/\sum_i p_i(I_i^{obs})^2]}$ with $p_i = 1/\sigma_i^2$.

Domain	1		2	
Propagation vector	$\boldsymbol{k}_1$	$\boldsymbol{k}_1'$	$\boldsymbol{k}_2$	$\boldsymbol{k}_2'$
k_x	0.500	−0.500	0.500	−0.500
k_y	0.405	0.405	−0.405	−0.405
k_z	0.083	0.083	0.083	0.083
m_x^k (μ_B)	−0.042(4)	0.038(4)	0.039(4)	−0.040(4)
m_y^k (μ_B)	0.598(3)	0.582(3)	0.591(3)	0.593(4)
m_z^k (μ_B)	0	0	0	0
β (deg)	−4.0(0.4)	+3.7(0.4)	+3.8(0.4)	−3.9(0.4)
R	6.4%	6.5%	7.1%	8.1%

They lead to $\beta = -3.9(0.3)^\circ$.

The magnetic moment $\boldsymbol{m}(\boldsymbol{r})$ of the double-$\boldsymbol{k}$ structure is the sum of the Fourier components $\boldsymbol{m}^{\pm k}$ and $\boldsymbol{m}^{\pm k'}$. It reads

$$\boldsymbol{m}(\boldsymbol{r}) = 2|\boldsymbol{m}^k|\cos(2\pi\boldsymbol{k}\cdot\boldsymbol{r})\boldsymbol{u} + 2|\boldsymbol{m}^{k'}|\cos(2\pi\boldsymbol{k}'\cdot\boldsymbol{r} - \Delta\phi)\boldsymbol{u}' \tag{1}$$

where $\Delta\phi$, the phase difference between the two Fourier components $\boldsymbol{m}^k$ and $\boldsymbol{m}^{k'}$, cannot be determined experimentally. $\boldsymbol{u}$ and $\boldsymbol{u}'$ are the unit vectors in the directions of $\boldsymbol{m}^k$ and $\boldsymbol{m}^{k'}$ respectively. Because of the relation between $\boldsymbol{m}^k$ and $\boldsymbol{m}^{k'}$, the moment components are

$$m_x(\boldsymbol{r}) = 2m_x^k[\cos(2\pi\boldsymbol{k}\cdot\boldsymbol{r}) - \cos(2\pi\boldsymbol{k}'\cdot\boldsymbol{r} - \Delta\phi)] \tag{2}$$

$$m_y(\boldsymbol{r}) = 2m_y^k[\cos(2\pi\boldsymbol{k}\cdot\boldsymbol{r}) + \cos(2\pi\boldsymbol{k}'\cdot\boldsymbol{r} - \Delta\phi)]. \tag{3}$$

Because $\boldsymbol{k} - \boldsymbol{k}' = (1\ 0\ 0)$, they can also be written as

$$m_x(\boldsymbol{r}) = -4m_x^k\sin(\pi r_x + \Delta\phi/2)\sin(2\pi\boldsymbol{k}\cdot\boldsymbol{r} - (\pi r_x + \Delta\phi/2)) \tag{4}$$

$$m_y(\boldsymbol{r}) = +4m_y^k\cos(\pi r_x + \Delta\phi/2)\cos(2\pi\boldsymbol{k}\cdot\boldsymbol{r} - (\pi r_x + \Delta\phi/2)). \tag{5}$$

The magnetic moment will be along $\boldsymbol{b}$ if $m_x(\boldsymbol{r}) = 0$, i.e. $\sin(\pi r_x + \Delta\phi/2) = 0$, or $\Delta\phi = -2\pi r_x(2\pi)$. Because of the body-centred structure of $CeNi_2Al_5$, this condition cannot be fulfilled simultaneously by atoms at the corners of the cells (integer values of r_x) and by atoms at the centres of the cells (half-integer values of r_x). Thus no value of $\Delta\phi$ can lead to moments along $\boldsymbol{b}$ on all the cerium atoms.

If we admit that $m_x \neq 0$, the expressions for m_x, equation (4), and m_y, equation (5), show that in the ($\boldsymbol{a}$, $\boldsymbol{b}$) plane of the body-centred structure of $CeNi_2Al_5$, the Ce moment describes an ellipse, with axes $\boldsymbol{x}$ and $\boldsymbol{y}$ and with maximum amplitudes

$$m_{x_0} = |4m_x^k\sin(\pi r_x + \Delta\phi/2)| \qquad m_{y_0} = |4m_y^k\cos(\pi r_x + \Delta\phi/2)|.$$

This can be written as follows:

for corner atoms ($r_x = n$):

$$m_{x_0} = |4m_x^k\sin(\Delta\phi/2)| \qquad m_{y_0} = |4m_y^k\cos(\Delta\phi/2)|$$

for centre atoms ($r_x = n + 1/2$):

$$m_{x_0'} = |4m_x^k\cos(\Delta\phi/2)| \qquad m_{y_0'} = |4m_y^k\sin(\Delta\phi/2)|.$$

If $\Delta\phi = 0$ (or π), the two ellipses transform themselves into two sinusoids:

- for corner atoms: one sinusoid along $\boldsymbol{b}$ (or $\boldsymbol{a}$) with maximum amplitude $|4m_y^k|$ (or $|4m_x^k|) = 2.39\ \mu_B$ (or $0.16\ \mu_B$);
- for centre atoms: one sinusoid along $\boldsymbol{a}$ (or $\boldsymbol{b}$) with maximum amplitude $|4m_x^k|$ (or $|4m_y^k|) = 0.16\ \mu_B$ (or $2.39\ \mu_B$).

Such configurations are very unlikely, because 50% of the moments would be oriented along the $\boldsymbol{a}$-direction. However, the moment value along that direction would remain very small, because of the strong anisotropy due to the CEF effects. Besides, the maximum moment along $\boldsymbol{b}$ ($2.39\ \mu_B$) would be higher than that reached in the highest applied magnetic fields ($1.7\ \mu_B$) and even higher than the moment of the Ce^{3+} free ion ($2.14\ \mu_B$). Furthermore, the two Ce in the cell would not behave in the same way, although they belong to the same Bravais lattice.

In contrast, if $\Delta\phi = \pm\pi/2$, the moments of the two types of atom describe identical ellipses, with axes

$$m_{x_0} = m_{x_0'} = 2\sqrt{2}|m_x^k| = 0.11(1)\ \mu_B$$
$$m_{y_0} = m_{y_0'} = 2\sqrt{2}|m_y^k| = 1.69(1)\ \mu_B.$$

For $\Delta\phi = +\pi/2$, the moment components are

for corner atoms:	$m_x(\boldsymbol{r}) = +0.11\sin t$	$m_y(\boldsymbol{r}) = +1.69\cos t$
for centre atoms:	$m_x(\boldsymbol{r}) = -0.11\cos t$	$m_y(\boldsymbol{r}) = -1.69\sin t$

with

$$t = 2\pi\boldsymbol{k}\cdot\boldsymbol{r} - \pi/4.$$

The maximum value of the moment is very close to that obtained from the magnetization measurements ($1.7\ \mu_B$). With this solution the moments are not along the easy-magnetization direction $\boldsymbol{b}$, but describe a very flat ellipse ($x_0/y_0 = m_x^k/m_y^k \approx 1/15$). However, most of the moments are very close to $\boldsymbol{b}$. The percentage of moments within an angle α_0 with the $\boldsymbol{b}$-direction is drawn versus α_0 in figure 3. For instance, 77% of the moments lie within $\alpha_0 = 10^\circ$. Furthermore, as the moment deviates from the $\boldsymbol{b}$-direction, its amplitude decreases rapidly as shown by its variation (figure 4) versus its angle α with $\boldsymbol{b}$. Its value is divided by a factor of two for $\alpha = 6.5^\circ$ only.

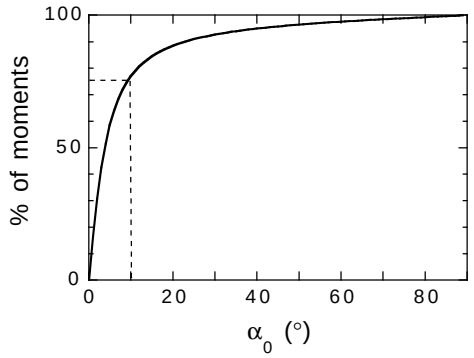

Figure 3. The percentage of moments within an angle α_0 with the $\boldsymbol{b}$-direction, versus α_0.

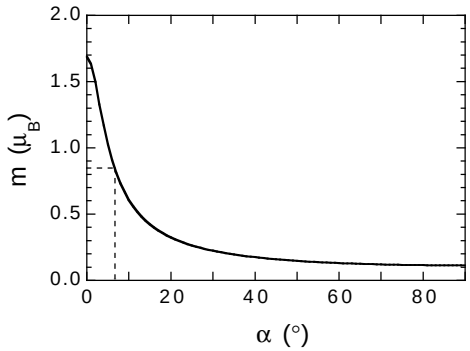

Figure 4. The amplitude m of the moment as a function of its angle α with the $\boldsymbol{b}$-direction.

The magnetic structure and the ellipsoidal variation of the moment in the ($\boldsymbol{a}$, $\boldsymbol{b}$) plane are shown in figures 5(a) and 5(b), respectively. The compound is purely antiferromagnetic in the $\boldsymbol{a}$-direction ($k_x = 1/2$). Figure 6 shows the propagation along the $\boldsymbol{c}$-direction. The moment describes elliptic helices with a periodicity of 12 cells ($k_z = 0.083 = 1/12$) and one can notice that the overall structure is a non-chiral spiral, as the moments for corner and centre atoms rotate in opposite senses.

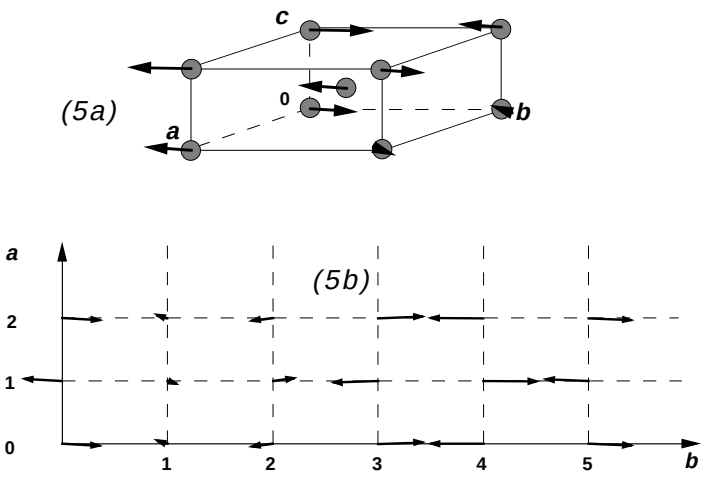

Figure 5. The magnetic structure of $CeNi_2Al_5$. (a) The crystallographic unit cell. (b) Propagation in the ($\boldsymbol{a}$, $\boldsymbol{b}$) plane.

2.2. Complex Fourier components

As the magnetic structure finally obtained is not collinear, one can imagine that the Fourier component $\boldsymbol{m}^k$ that we have refined could be not real. In fact, $\boldsymbol{m}^k$ being a complex vector represents the most general solution. For the single-$\boldsymbol{k}$ case, it corresponds to a helical structure based on ellipses instead of a collinear sine-wave-modulated structure. We tried refinements in which $m_x^k = M_x^k(\cos\psi_x + \mathrm{i}\sin\psi_x)$ and $m_y^k = M_y^k(\cos\psi_y + \mathrm{i}\sin\psi_y)$ are complex. The

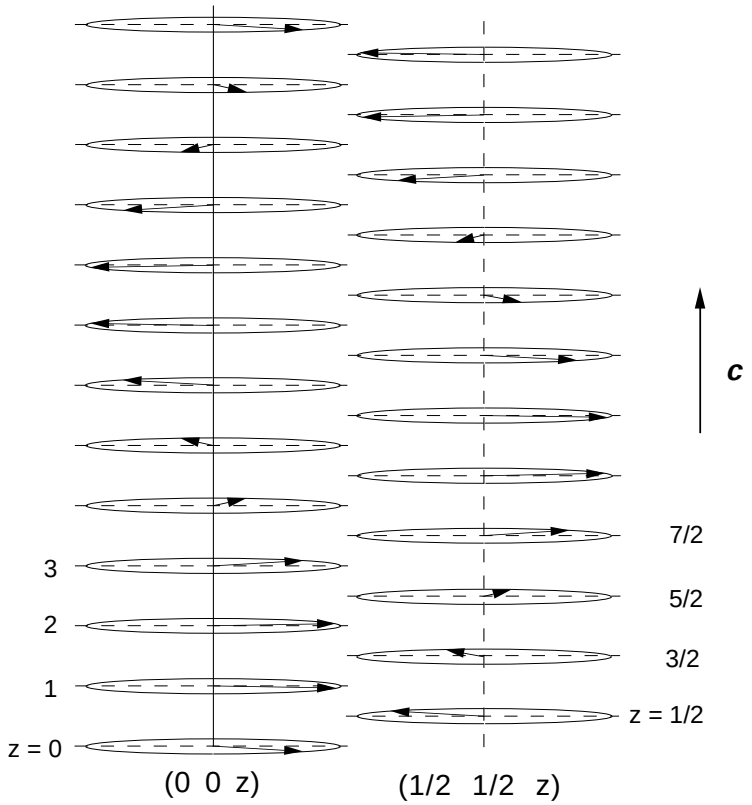

Figure 6. Propagation along the $\boldsymbol{c}$-direction. The moment describes ellipses which are located in the ($\boldsymbol{a}$, $\boldsymbol{b}$) plane, perpendicular to the propagation direction $\boldsymbol{c}$.

reliability factor of a first refinement with m_x^k purely real and m_y^k purely imaginary (an ellipse with axes along $\boldsymbol{x}$ and $\boldsymbol{y}$) is $R = 11.7\%$ for the propagation vector $\boldsymbol{k}_1$, which is less good than the one found previously (6.4%; see table 1). However, a second refinement with both components complex ($M_x^k = -0.110(7)$, $M_y^k = 0.588(3)$ and $\psi_y - \psi_x = 66(2)^\circ$) gives a better reliability factor, $R = 4.5\%$. In the single-$\boldsymbol{k}$-case, the moment is located on ellipses with their larger axes $\boldsymbol{y}_0$ at -4.4° from $\boldsymbol{b}$ and with an axis ratio $x_0/y_0 = 0.17$. The coupling of the two propagation vectors $\boldsymbol{k} = (0.500, 0.405, 0.083)$ and $\boldsymbol{k}' = (-0.500, 0.405, 0.083)$ leads to a moment located on ellipses with their larger axes $\boldsymbol{Y}_0$ at + or -9.8° from $\boldsymbol{b}$ for corner and centre atoms, respectively. The axis ratio is $X_0/Y_0 = 0.07$, with $Y_0 = 1.68(1)\ \mu_B$. In this final structure, the moment describes the same ellipses as for the previous structure obtained with $\boldsymbol{m}^k$ real, the only difference being in the orientation of these ellipses. For $\boldsymbol{m}^k$ real the axis of the ellipses are along $\boldsymbol{x}$ and $\boldsymbol{y}$, whereas for $\boldsymbol{m}^k$ complex the ellipses are tilted $+10^\circ$ away from $\boldsymbol{b}$ for one half of the atoms and tilted -10° for the second half. In this case, the maximum moment along the $\boldsymbol{b}$-direction would be $1.68 \cos 10^\circ = 1.66(1)\ \mu_B$.

The two solutions, the real one and the complex one, are very close, but the first one corresponds to a macroscopic moment in slightly better agreement with the saturation magnetization ($1.7\ \mu_B$). For the sake of simplicity, we shall choose in the following sections the first solution, assuming that $\boldsymbol{m}^k$ is a real vector.

3. Evolution of the magnetic structure at 0.4 K

For Kramers ions such as Ce ($J = 5/2$), modulated structures are not stable at very low temperatures and are generally expected to evolve towards a constant-moment-type structure [12]. One interesting point is then to look at the evolution of the magnetic structure of $CeNi_2Al_5$ as temperature decreases—in particular to check whether the Fourier component $\boldsymbol{m}^k$ tends to align along $\boldsymbol{b}$ ($\beta \longrightarrow 0$), and whether any satellites corresponding to higher-order harmonics can be observed. In the simple case of a sine-wave-modulated function which transforms itself into a square-type function, reflections corresponding to propagation vectors $3\boldsymbol{k}$, $5\boldsymbol{k}$, ... will appear with intensities 1/9, 1/25, ... of those of the first-order magnetic reflections, respectively.

A dilution cryostat [13] was mounted on D10. At the lowest temperature that could be reached (0.4 K), the intensities of the first-order magnetic satellites were measured. The refinement then leads to slightly increased values (≈15%) of the Fourier components $\boldsymbol{m}^k$ and especially to an unchanged value of β within the experimental accuracy ($\beta = -3.9(0.5)^\circ$).

We have also found third-order satellites and we have been able to measure 20 of them at $T = 0.4$ K (see, for instance, reflection (1 0 1) $- 3\boldsymbol{k}$ in figure 7). Their intensities are very small and the refinement of the corresponding Fourier components $\boldsymbol{m}^{3k}$ is quite inaccurate. In particular, the component m_x^{3k} is smaller than its error bar and one cannot tell whether $\boldsymbol{m}^{3k}$ is parallel to $\boldsymbol{m}^k$ or aligned along $\boldsymbol{b}$. In the case of our double-$\boldsymbol{k}$ structure, the combination of higher-order terms in the Fourier development with appropriate phase differences can give rise to a magnetic structure with most of the moments along $\boldsymbol{b}$, with their maximum value, and fewer moments close to $\boldsymbol{a}$. As above, these phase differences cannot be determined from the experimental data.

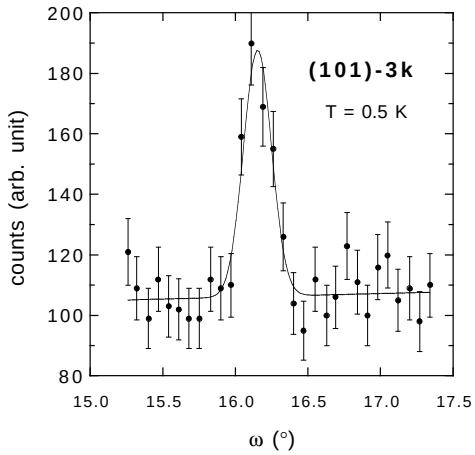

Figure 7. The intensity of the (1 0 1) $- 3\boldsymbol{k}$ reflection at $T = 0.5$ K.

Figure 8(a) represents the thermal variation of the intensities of the two reflections (1 0 1) $- \boldsymbol{k}$ and (1 0 1) $- 3\boldsymbol{k}$. They seem to appear a little below $T_N = 2.6$ K and increase together as temperature is lowered. But the $3\boldsymbol{k}$-satellite is very small compared to the $\boldsymbol{k}$-satellite. The ratio of their intensities is shown in figure 8(b). $I(3\boldsymbol{k})/I(\boldsymbol{k})$ is only 0.005 at 1.6 K and reaches 0.008 at 0.4 K, which is very far from the value of 1/9 (=0.111) expected for square-type structures. Because of the very small intensity of the $3\boldsymbol{k}$-satellites, the actual magnetic structure at 1.6 K is almost identical to that described above.

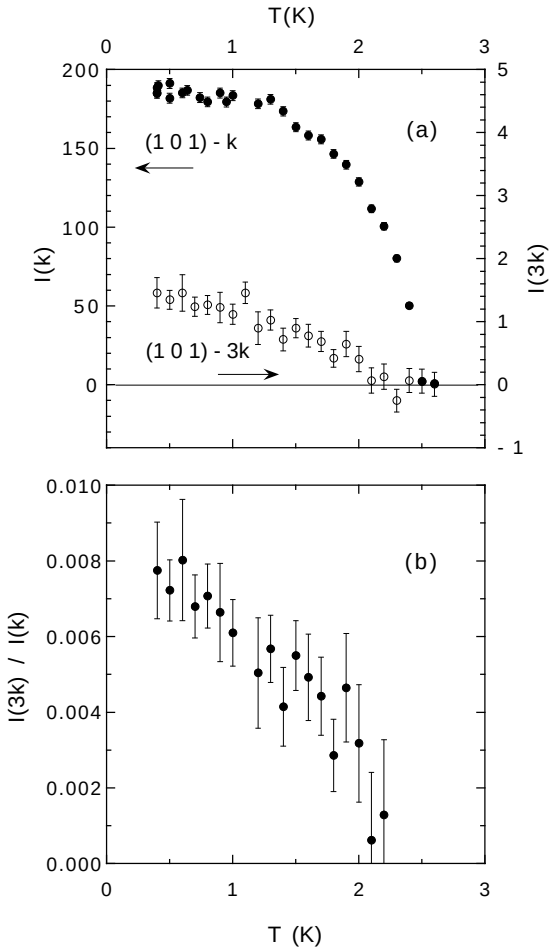

Figure 8. (a) Thermal variation of the intensities of the (1 0 1) $-\boldsymbol{k}$ and (1 0 1) $-3\boldsymbol{k}$ reflections. Note the two different scales. (b) Thermal variation of the ratio of their intensities $\boldsymbol{I}(3\boldsymbol{k})/\boldsymbol{I}(\boldsymbol{k})$.

4. Polarization analysis

In order to check the direction of the Fourier component $\boldsymbol{m}^k$, polarization analysis experiments were performed at ILL using CRYOPAD [14] on IN20. The three components of the polarization of the diffracted beam $\boldsymbol{P}'$ were measured for different orientations of the incoming polarization $\boldsymbol{P}$. Three directions of the latter were explored: parallel to the scattering vector $\boldsymbol{q}$ ($\boldsymbol{P}_{\text{front}}$), perpendicular to $\boldsymbol{q}$ in the scattering plane ($\boldsymbol{P}_{\text{left}}$) and orthogonal to the scattering plane (i.e. vertical) ($\boldsymbol{P}_{\text{up}}$). For the measurement, the crystal was oriented with its [1 0 $\bar{6}$] axis vertical and with the scattering vector of reflection (-0.5, -0.405, -0.083) (=(0 0 0) $-\boldsymbol{k}$) in the horizontal plane. The sample was cooled down to 1.3 K in a cryostat.

According to Blume's formula [15], in a magnetic structure where $\boldsymbol{F}_M^\star$ is parallel to $\boldsymbol{F}_M$, the polarization vector $\boldsymbol{P}$ rotates by half a turn around $\boldsymbol{F}_{M\perp}$ (the component of $\boldsymbol{F}_M$ perpendicular to the scattering vector) during the scattering process of a purely magnetic reflection. The direction of the scattered polarization $\boldsymbol{P}'$ depends then on the direction of $\boldsymbol{F}_{M\perp}$, or $\boldsymbol{m}_\perp^k$

here—that is on the angle β of $\boldsymbol{m}^k$ with the $\boldsymbol{b}$-direction in the ($\boldsymbol{a}$, $\boldsymbol{b}$) plane. $\boldsymbol{P}'$ has been calculated for this experimental arrangement and for the three different incident polarizations described above. Its angle θ with the vertical axis is 90°, independent of β for $\boldsymbol{P}_{\text{front}}$. For $\boldsymbol{P}_{\text{up}}$ and $\boldsymbol{P}_{\text{left}}$, the calculated θ-value is drawn as a function of β in figures 9(a) and 9(b), respectively.

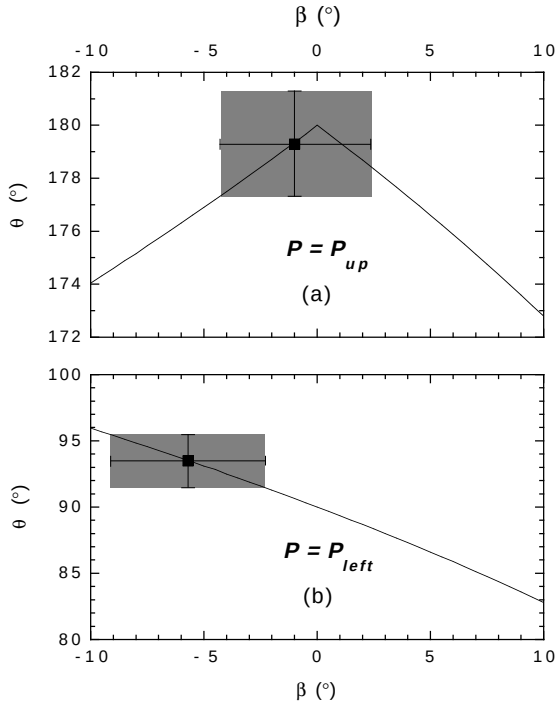

Figure 9. The θ-angle with the vertical axis [1 0 $\bar{6}$] of the polarization scattered on the reflection (-0.5, -0.405, -0.083) for the following incident polarizations: (a) $\boldsymbol{P}_{\text{up}}$; (b) $\boldsymbol{P}_{\text{left}}$.

Measurements of $\boldsymbol{P}'$ at various temperatures between 1.3 K and 2.3 K show no temperature dependence. The experimental values found for θ are

$$\theta(\boldsymbol{P}_{\text{front}}) = 90.6(2.0)^\circ \qquad \theta(\boldsymbol{P}_{\text{up}}) = 179.3(2.0)^\circ \qquad \theta(\boldsymbol{P}_{\text{left}}) = 93.5(2.0)^\circ.$$

The error bars of 2° on θ are due to the uncertainty in determining the zeros. The $\boldsymbol{P}_{\text{front}}$-value is in agreement with the calculation. The two others are reported on the β-dependence curves of figures 9(a) and 9(b). From the $\boldsymbol{P}_{\text{left}}$-result, it can be deduced that β has a negative value and, from the combination of the two $\boldsymbol{P}_{\text{up}}$- and $\boldsymbol{P}_{\text{left}}$-results, β has been estimated to be $-3.4(2.4)^\circ$.

5. Conclusions

These new measurements on $CeNi_2Al_5$ (classical diffraction with higher resolution, very-low-temperature diffraction, polarization analysis) confirm the result previously found, that the Fourier component $\boldsymbol{m}^k$ of the magnetic moment $\boldsymbol{m}$ is not oriented along the easy-magnetization direction $\boldsymbol{b}$ but is tilted towards $\boldsymbol{a}$ in the ($\boldsymbol{a}$, $\boldsymbol{b}$) plane. The tilt angle ($\approx 4^\circ$) is given by the experiment on the four-circle diffractometer at a large wavelength. The value deduced from the

three-dimensional polarization analysis supports the value obtained from classical diffraction. This angle remains unchanged as the temperature is lowered down to 0.4 K.

The proposed double-$\boldsymbol{k}$ structure, with a phase difference of $\pi/2$ between the Fourier components $\boldsymbol{m}^k$ and $\boldsymbol{m}^{k'}$, is a non-chiral spiral. The resulting moment describes very flat ellipses in the ($\boldsymbol{a}$, $\boldsymbol{b}$) plane, with their large axis along the $\boldsymbol{b}$-direction. The axis ratio is given by the ratio

$$m_x^k/m_y^k = \tan 4^\circ.$$

As already observed from the low-temperature nuclear orientation experiments [9], the moment $\boldsymbol{m}$ is not along $\boldsymbol{b}$. It is in fact oriented in all of the directions of the ($\boldsymbol{a}$, $\boldsymbol{b}$) plane, but most of the moments are very close to $\boldsymbol{b}$ and the moment amplitude decreases drastically as the moment moves away from $\boldsymbol{b}$. Its maximum value is equal to that obtained by magnetization measurements above 10 T. The two Ce atoms in the unit cell play the same role, which is consistent with the absence of crystalline distortion. For the propagation along $\boldsymbol{c}$, their moments rotate in opposite senses.

There is a strong parallel between the magnetic structure of $CeNi_2Al_5$ which has been determined here and that of the compound $CeAl_2$. In both structures one can identify two equivalent positions for the Ce atoms. In $CeAl_2$, they are the two positions of the diamond structure ((0, 0, 0) and (1/4, 1/4, 1/4)). In $CeNi_2Al_5$, they are the origin and the centre of the orthorhombic cell. In both cases an incommensurate propagation vector has been found for the magnetic structure, (0.612, 0.388, 0.500) for $CeAl_2$ [16] and (0.500, 0.405, 0.083) for $CeNi_2Al_5$ [5]. In both cases, the investigation of the magnetic reflections with a magnetic field applied to the sample has revealed that the magnetic structure is double $\boldsymbol{k}$, which means that the Fourier components $\boldsymbol{m}^k$ and $\boldsymbol{m}^{k'}$, corresponding to two equivalent propagation vectors $\boldsymbol{k}$ and $\boldsymbol{k}'$, couple together to generate the actual magnetic structure (see [17] for $CeAl_2$ and [6] for $CeNi_2Al_5$). As the phase difference between $\boldsymbol{m}^k$ and $\boldsymbol{m}^{k'}$ is not given by the neutron experiment, in both cases this phase difference has been guessed on physical grounds, relying in particular on the fact that the two Ce positions must be equivalent in the magnetic structure. Finally, in both cases, this magnetic structure corresponds to two magnetic helices, one helix for each Ce position, rotating in opposite directions, in order to give a non-chiral magnetic structure.

The differences which exist in the magnetic anisotropies of the two compounds induce however differences in the magnetic helices. In $CeAl_2$, the Ce^{3+} ions have a cubic symmetry with weak magnetic anisotropy. It results in elliptic helices with a weak ellipticity. Just below T_N, the ratio between the two ellipse axes is equal to tan 35° which corresponds to a variation of the moment amplitude of 30%. As temperature decreases, the helices become more and more circular [18]. The resulting moment modulation has been extrapolated to 15% at 0 K and these remaining variations have been attributed to the Kondo effect. In contrast, in $CeNi_2Al_5$ the Ce^{3+} ions have an orthorhombic symmetry with a very high magnetic anisotropy. The resulting helices are very flat, with a ratio of 15 between the largest and the smallest moments. These variations are clearly due to the crystal electric field. As temperature goes down, third-order satellites appear and increase, indicating a change in the shape of the helices with more larger and fewer smaller moments. In both compounds, in spite of their differences, the moments tend to reduce their variations at low temperature, but the Kondo effect is still present.

References

[1] Isikawa Y, Mizushima T, Oyabe K, Mori K, Sato K and Kamigaki K 1991 *J. Phys. Soc. Japan* **60** 1869

[2] Isikawa Y, Mori K, Kamigaki K, Mizushima T, Oyabe K, Ueda S and Sato K 1992 *J. Magn. Magn. Mater.* **108** 157

[3] Zarechnyuk O S, Yanson T I and Rykhal R M 1983 *Izv. Akad. Nauk SSSR, Met.* **4** 192
[4] Parthé E and Chabot B 1984 *Handbook on the Physics and Chemistry of Rare Earths* vol 6, ed K A Gschneidner Jr and L Eyring (Amsterdam: North-Holland) p 113
[5] Isikawa Y, Mizushima T, Sakurai J, Mori K, Muñoz A, Givord F, Boucherle J X, Voiron J, Oliveira I S and Flouquet J 1994 *J. Phys. Soc. Japan* **63** 2349
[6] Boucherle J X, Burlet P, Givord F, Isikawa Y, Neudert R, Schmitt D and Schober H 1995 *J. Phys.: Condens. Matter* **7** 8337
[7] Boucherle J X, Givord F, Schweizer J and Isikawa Y 1997 *Physica* B **234–236** 875
[8] Isikawa Y, Mori K, Mizushima T, Sakurai J, Muñoz A, Givord F, Boucherle J X, Flouquet J and Oliveira I S 1994 *Physica* B **194–196** 373
[9] Nishimura K, Oliveira I S, Stone N J, Richards P, Ohya S, Isikawa Y and Mori K 1993 *Physica* B **186–188** 400
[10] Givord F, Boucherle J X and Isikawa Y 1996 *J. Phys. Soc. Japan Suppl.* B **65** 129
[11] Wolfers P 1990 *J. Appl. Crystallogr.* **23** 554
[12] Gignoux D, Lemaire R and Paccard D 1972 *Phys. Lett.* A **41** 187
[13] Pujol S 1994 *Thesis* University of Grenoble
[14] Brown P J, Forsyth J B and Tasset F 1993 *Proc. R. Soc.* A **442** 147
[15] Blume M 1963 *Phys. Rev.* **130** 1670
[16] Barbara B, Boucherle J X, Rossignol M F, Schweizer J and Buevoz J L 1979 *J. Appl. Phys.* **50** 2300
[17] Forgan E M, Rainford B D, Lee S L, Abell J S and Bi Y 1990 *J. Phys.: Condens. Matter* **2** 10 211
[18] Givord F, Schweizer J and Tasset F 1997 *Physica* B **234–236** 685